# CONTACTING AND RECOMBINATION ANALYSIS OF BORON EMITTERS VIA ETCH-BACK FOR ADVANCED N-TYPE SI SOLAR CELLS

Yvonne Schiele, Giso Hahn, Barbara Terheiden
University of Konstanz, Department of Physics, P.O. Box 676, 78457 Konstanz, Germany
Phone: +49 (0) 7531 88 4995, Fax: +49 (0) 7531 88 3895, Email: Yvonne.Schiele@uni-konstanz.de

ABSTRACT: In p-type c-Si solar cells, selective emitter structures generated by emitter etch-back (EEB) have been introduced in recent years in order to minimize electrical losses in the phosphorous emitter being one of the dominant factors limiting the performance of standard screen-printed p-type c-Si solar cells. In this work, a homogeneously or selectively etched-back boron emitter is demonstrated to provide additional benefits yielding an enhanced conversion efficiency in n-type Si solar cells.
By means of subsequent B-EEB, contacting and recombination properties of B emitters dependent on their sheet resistance, surface concentration, and profile depth are studied indicating the latter to be the crucial parameter. Based on this, the characteristics of the optimal B emitter regarding low saturation current density and low specific contact resistivity are determined for the cases of homogeneous and selective etch-back.
By employing the selectively etched-back B emitter in initial solar cells, a $V_{OC}$ gain of 5 mV and a significant shunting reduction compared with homogeneously doped devices is achieved.
Keywords: n-type, Boron, Etch-back

## 1 INTRODUCTION

Solar cells based on n-type crystalline silicon (c-Si) wafers have raised growing interest (e.g. [1-4]) not only since several record efficiencies above 25% have been attained with n-type Si substrate material recently [5-7]. Replacing p-type Si wafers, predominantly used in current solar cell production, by n-type Si material provides various benefits: n-type solar cells can generally attain higher conversion efficiencies since minority carrier lifetimes are less affected by certain impurities [8] and their efficiency does not suffer B-O complex related light induced degradation [9].

Despite these benefits, n-type Si substrate material has not replaced p-type Si in the majority yet which is not least due to the difficulty to attain a well passivated and at the same time well contacted boron emitter.

In p-type c-Si solar cells, however, selective emitters have been introduced in recent years in order to minimize electrical losses in the P emitter being one of the dominant factors limiting the performance of standard screen-printed p-type c-Si solar cells.

In n-type solar cells, a selective B emitter is expected to provide additional benefits yielding enhanced conversion efficiency. Within this study, such selective B emitters are generated by a single $BBr_3$ diffusion process followed by a wet-chemical partial and selective etch-back of the heavily doped $p^+$ layer via porous Si formation (B-EEB) [10]. Besides the generation of a selective emitter, this technique allows, also homogeneously, to systematically modify the diffused emitter profile. Thus, B-EEB may provide the following benefits:

A) With selective B emitters, the trade-off between high surface doping concentration [$B_{surf}$] to achieve low specific contact resistivity $\rho_C$ and high emitter sheet resistance $R_{sh}$ to minimize emitter saturation current density $j_{0e}$ necessary with homogeneous emitters can be circumvented.

B) Deeper emitter profiles can be employed below the metal contacts in order to avoid the shunting of the p-n junction which impairs solar cell efficiency and applies especially to co-fired Ag/Al paste because of Al spiking into the emitter [11].

C) Like for higher [$B_{surf}$] (cf. A), employing a deeper B emitter profile beneath the metal contacts may additionally yield lower $\rho_C$ [12]. Furthermore, the deeper B emitter may also yield enhanced shielding of the highly recombinative contacts.

D) Due to the higher solubility of B in $SiO_x$ than in Si, the $BBr_3$ emitter profile typically exhibits a [B] depletion towards the wafer surface which is identified to cause increased surface recombination [13]. This can be eliminated by removing the depleted layer by means of boron emitter etch-back.

E) Despite an oxidation step during $BBr_3$ diffusion, the borosilicate glass (BSG) layer may be hard to remove in HF solution. B-EEB as part of the solar cell process may reliably etch off the BSG due to $HNO_3$ added to HF. A completely removed BSG permits better passivation of the B emitter beneath.

For a high performance n-type solar cell, it is crucial to know and implement the optimal B emitter profile. In this study, the B-EEB process is used to create B emitters with various surface doping concentrations [$B_{surf}$] and profile depths, i.e. $R_{sh}$, based on different starting $BBr_3$ emitters. Thus, these three emitter parameters are uncoupled and their influence on emitter characteristics as emitter saturation current density $j_{0e}$ and specific contact resistivity $\rho_C$ can be investigated.

With the attained correlations, the optimal selective emitter is identified as well, featuring low $j_{0e}$ in the etched-back regions and low $\rho_C$ beneath the metal contacts.

## 2 BORON EMITTER ETCH-BACK

For p-type solar cells, the technical implementation of a selective $n^+$ emitter by wet chemical etch-back via porous Si (por-Si) formation and subsequent removal of the porous layer was introduced by Haverkamp et al. [14]. This approach permits a good controlling of porous layer thickness, i.e. target $R_{sh}$.

Since the underlying chemical reactions are dependent on the concentration of valence band holes at the Si surface, the B-EEB solution needs to be adjusted for $p^+$ emitters regarding the following requirements:

- homogeneous etching on a large-area Si wafer
- controllable and adjustable etching rate and target emitter $R_{sh}$ along with maintaining reasonable process duration.

Etching Si in the acidic EEB solution composed of HF, $HNO_3$ and $H_2O$ (stain etching), spots on the Si surface randomly become oxidation or reduction sites acting as localized electrochemical cells and sustaining currents on the surface. The oxidation on an anodic site consists in

$$Si^0 + 2H_2O + m\,h^+ \rightarrow SiO_2 + 4H^+ + (4-m)e^- \qquad (1)$$

while the reduction on a cathodic site is

$$HNO_3 + 3H^+ \rightarrow NO + 2H_2O + 3h^+. \qquad (2)$$

Por-Si formation is initiated by valence band holes at the Si surface (cf. eq. 1) being products of the reduction (eq. 2). Thus, the injection of $h^+$ into the valence band is the crucial role of the oxidant and its electrochemical potential is a control parameter to influence por-Si formation. $HNO_3$-rich stain etch solutions induce electropolishing, whereas in HF-rich solutions, the process is limited by the availability of holes, thus por-Si is formed [15].

Using an adapted etching solution with modified concentrations of the chemicals, the BSG layer is removed reliably and faster whereupon the B emitter is etched-back homogeneously and in a controllable manner [10].

## 3 EXPERIMENTAL

In this work, $j_{0e}$ and $\rho_C$ are investigated on planar $p^+$ doped Si wafer surfaces as they occur in rear emitter n-type solar cells. Corresponding investigations on textured surfaces for front emitters are subjected to further studies. The metal contact to the B emitter is established by evaporated Al (PVD).

The $j_{0e}$ and $\rho_C$ sample structure (Fig. 2b & 2c) and their processing sequence (Fig. 1) are similar to the ones of the solar cell (Fig. 2a) where the selective B emitter is to be employed. This n-type solar cell features a $SiO_2/SiN_x$ passivated P front surface field (FSF) contacted by a screen-printed Ag grid and an $Al_2O_3/SiN_x$ passivated homogeneous or selective B emitter at the planar rear. The $Al_2O_3/SiN_x$ passivation is opened locally where the contact to the emitter is established. For a monofacial solar cell, the Al is evaporated on full-area, in case of a bifacial concept, a finger grid structure is deposited.

The novel B-EEB step is inserted into the process after high temperature $POCl_3$ diffusion and thermal oxidation which modify the $BBr_3$ diffused emitter and cause an extra [B] depletion at the wafer surface.

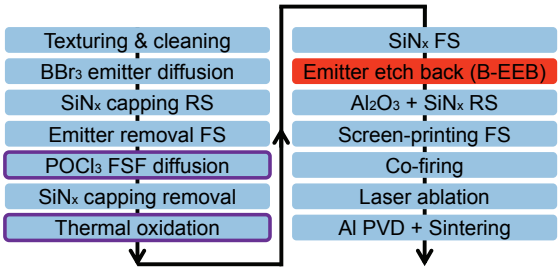


**Figure 1:** Processing sequence of the described n-type solar cell with passivated selective rear emitter, passivated FSF and evaporated Al rear contacts.

For the symmetrical $j_{0e}$ samples (Fig. 2b), planar 200 Ωcm n-type FZ-Si (250 µm thick) are used. The emitter is created by $BBr_3$ diffusion and passivated by a fired $Al_2O_3/SiN_x$ stack after B-EEB. The B emitter of the alkaline-etched n-type Cz-Si (2 Ωcm) $\rho_C$ samples (Fig. 2c) is contacted by electron beam evaporated and sintered Al fingers.

$j_{0e}$ is determined from photoconductance decay measurement evaluated at an injection level of $\Delta n = 1\times10^{16}$ cm$^{-3}$ (high level injection mode) [16] using a Sinton lifetime tester. $\rho_C$ is measured by the transfer length method. $R_{sh}$ of the B emitters is determined by four-point probe and their depth profile by electrochemical capacitance voltage (ECV) measurement.

In order to examine the potential benefits (A - E in sec. 1) of homogeneously or selectively etched-back B emitters, different starting emitters are subsequently etched-back to various depths, creating different $[B_{surf}]$ and profile depths yielding an $R_{sh}$ range of ~30 to ~190 Ω/sq.

## 4 RESULTS & DISCUSSION

Fig. 3a depicts exemplarily the 30 Ω/sq $BBr_3$ diffused emitter profiles before and after the high temperature steps of the solar cell process as well as the profiles subsequently etched-back to different $R_{sh}$. The high temperature steps modify the emitter profile towards a more depleted $[B_{surf}]$. By means of B-EEB, the [B] depleted region can be removed completely.

The influence of $R_{sh}$, profile depth and $[B_{surf}]$ on $j_{0e}$ and $\rho_C$ is depicted in Fig. 3b-f. Despite the continuous $j_{0e}$ decrease with higher $R_{sh}$ of the non-etched-back emitters, no general $j_{0e} - R_{sh}$ dependency is observed (Fig. 3b). $j_{0e}$ is rather determined by profile depth (Fig. 3c), whereas $j_{0e}$ does not exhibit an explicit dependency on $[B_{surf}]$ (not shown). Fig. 3d demonstrates the clear trend of $\rho_C$ with $R_{sh}$, independent of B-EEB application. The dependency is caused by a $\rho_C$ decrease with increasing profile depth (Fig. 3e). $[B_{surf}]$, however, exhibits only a dependency within the etched-back or non-etched-back samples, respectively (Fig. 3f).

A further reduction of $j_{0e}$ by a better BSG removal in the B-EEB solution is not found (cf. E in sec. 1) as the BSG on the planar samples could already be completely etched off in HF. This may be different for textured surfaces and is still under investigation.

The correlation of an increased surface recombination due to the [B] depletion at the surface (cf. D in sec. 1) as it was observed in [13] could not be confirmed.

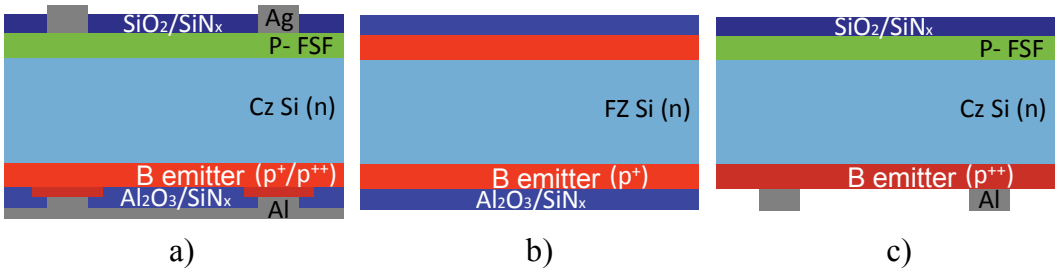


**Figure 2:** Cross sections of the investigated test structures: a) monofacial solar cell with selective rear emitter, b) $j_{0e}$ sample, c) $\rho_C$ sample.

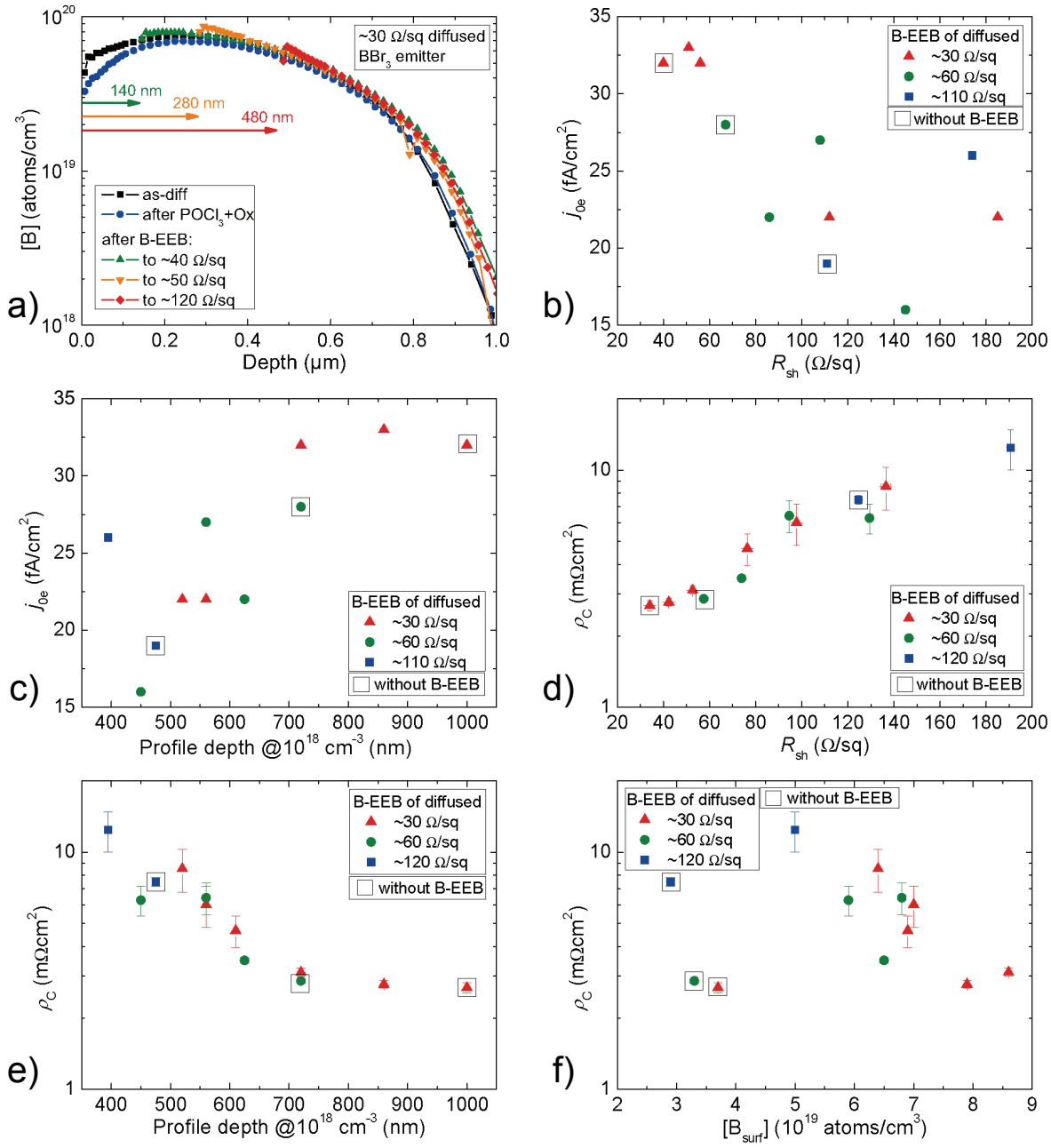


**Figure 3:** a) ECV profile of the 30 Ω/sq $BBr_3$ diffused emitter at different stages of the solar cell process (cf. Fig. 1). b)-f) Influence of $R_{sh}$, profile depth and $[B_{surf}]$ on $j_{0e}$ and $\rho_C$.

However, the results depicted in Fig. 3 demonstrate the benefits of the B-EEB process in achieving both low $\rho_C$ and low $j_{0e}$ (cf. A & C in sec. 1) having been proven right. Using a homogeneous emitter, a good compromise of $\rho_C = 3.5$ mΩcm$^2$ and $j_{0e} = 22$ fA/cm$^2$ can be attained for the 60 Ω/sq emitter etched-back to $R_{sh} \approx 80$ Ω/sq.

By employing a selective emitter in the n-type solar cell to achieve the optimal combination regarding low $j_{0e}$ between and low $\rho_C$ beneath the metal contacts, a ~60 Ω/sq starting B emitter has to be etched-back to ~140 Ω/sq ($j_{0e} = 16$ fA/cm$^2$, $\rho_C = 2.9$ mΩcm$^2$) or a ~30 Ω/sq emitter to ~110 Ω/sq ($j_{0e} = 22$ fA/cm$^2$, $\rho_C = 2.7$ mΩcm$^2$). However, further solar cell performance relevant parameters such as lateral conductivity are disregarded here.

Moreover, additional starting B emitters with certain profile shapes leading to further combinations of profile depth and [$B_{surf}$] before and after B-EEB can be designed which may yield even lower $j_{0e}$ and $\rho_C$ beneath and between the contacts, respectively.

Initial solar cells with selectively doped $p^+$ structures ($R_{sh} \approx 30$ Ω/sq + B-EEB to ~110 Ω/sq) are compared to homogeneously doped, non-etched-back devices ($R_{sh} \approx 50$ Ω/sq) [10]. By employing the selectively etched-back B emitter, a $V_{OC}$ gain of 5 mV is achieved along with maintaining $j_{SC}$. The benefit of a selective B emitter structure to reduce emitter shunting by Al spiking (cf. B in sec. 1) is also demonstrated as shunt resistance increases by a factor of 20 to 73 kΩcm$^2$ when employing a selective B emitter.

## 5 CONCLUSION & OUTLOOK

Within this study, a homogeneously or selectively etched-back boron emitter has been demonstrated to provide several benefits, which, if it is employed in n-type Si solar cells, yield an enhanced conversion efficiency:

- The trade-off between high surface doping concentration and/or deep emitter profile to achieve low contact resistivity and high sheet resistance to minimize emitter saturation current density can be circumvented.
- The [B] depleted region at the wafer surface can be removed completely.
- Employing deeper B emitter profiles below the metal contacts reduces the shunting of the p-n junction, provides enhanced shielding of the highly recombinative contacts, and yields a lower $\rho_C$.

Despite a continuous $j_{0e}$ decrease with higher $R_{sh}$ of non-etched-back emitters, no general $j_{0e} - R_{sh}$ dependency has been observed. $j_{0e}$ is rather determined by profile depth. A clear trend of $\rho_C$ with $R_{sh}$ independent of B-EEB application has been demonstrated and is caused by a $\rho_C$ decrease with increasing profile depth.

Using a homogeneously etched-back emitter ($R_{sh} \approx 60 \rightarrow 80$ Ω/sq), a good compromise of $\rho_C = 3.5$ mΩcm$^2$ and $j_{0e} = 22$ fA/cm$^2$ can be attained.

By employing a selective emitter to achieve the optimal combination regarding low $j_{0e}$ and $\rho_C$, a ~60 Ω/sq starting B emitter has to be etched-back between the contacts to ~140 Ω/sq or a ~30 Ω/sq emitter to ~110 Ω/sq yielding $j_{0e}$ of approx. 20 fA/cm$^2$ and $\rho_C$ below 3 mΩcm$^2$.

By employing the selectively etched-back B emitter ($R_{sh} \sim 30$ Ω/sq + B-EEB to ~110 Ω/sq) in initial solar cells, a $V_{OC}$ gain of 5 mV and a significant shunting reduction compared to homogeneously doped devices ($R_{sh} \sim 50$ Ω/sq) has been achieved [10].

The manufacturing of further types of solar cells and the extension of $j_{0e}$ and $\rho_C$ analysis to textured surfaces and screen-printed Ag/Al contacts regarding further n-type solar cell concepts is in progress.

## 6 ACKNOWLEDGEMENTS

The processing and characterization assistance of S. Joos is gratefully acknowledged. Part of this work was financially supported by the German Federal Ministry for the Environment, Nature Conservation and Nuclear Safety (FKZ 0325581). The content is the responsibility of the authors.

## 7 REFERENCES

[1] F. Kiefer, C. Ulzhöfer, T. Brendemühl, N.-P. Harder, R. Brendel, V. Mertens, S. Bordihn, C. Peters, J.W. Müller, IEEE J. Photov. 1 (1) (2011) 49.
[2] J. Benick, B. Hoex, M.C.M van de Sanden, W.M.M. Kessels, O. Schultz, S.W. Glunz, Appl. Phys. Lett. 92 (2008) 253504.
[3] F. Book, T. Wiedenmann, G. Schubert, H. Plagwitz, G. Hahn, En. Proc. 8 (2011) 487.
[4] H.-C. Chang, C.-J. Huang, P.-T. Hsieh, W.-C. Mo, S.-H. Yu, C.-C. Li, En. Proc. (2014), in print.
[5] D.D. Smith, P. Cousins, S. Westerberg, R. De Jesus-Tabajonda, G. Aniero, Y.-C. Shen, Proc. 40th IEEE PVSC (2014) 601, in print.
[6] J. Nakamura, N. Asano, T. Hieda, C. Okamoto, T. Ohnishi, M. Kobayashi, H. Tadokoro, R. Suganuma, Y. Matsumoto, H. Katayama, K. Higashi, T. Kamikawa, K. Kimoto, M. Harada, T. Sakai, H. Shigeta, T. Kuniyoshi, K. Tsujino, L. Zou, N. Koide, K. Nakamura, Proc. 40th IEEE PVSC (2014) 283, in print.
[7] K. Masuko, M. Shigematsu, T. Hashiguchi, D. Fujishima, M. Kai, N. Yoshimura, T. Yamaguchi, Y. Ichihashi, T. Mishima, N. Matsubara, T. Yamanishi, T. Takahama, M. Taguchi, E. Maruyama, S. Okamoto, Proc. 40th IEEE PVSC (2014) 191, in print.
[8] D. Macdonald, L.J. Geerligs, Appl. Phys. Lett. 85 (2004) 4061.
[9] S.W. Glunz, S. Rein, J.Y. Lee, W. Warta, J. Appl. Phys. 90 (2001) 2397.
[10] Y. Schiele, S. Joos, G. Hahn, B. Terheiden, En. Proc. (2014), in print.
[11] R. Lago, L. Pérez, H. Kerp, I. Freire, I. Hoces, N. Azkona, F. Recart, J.C. Jimeno, Prog. Photovoltaics: Res. Appl. 18 (2010) 20.
[12] S. Fritz, S. Riegel, S. Gloger, D. Kohler, M. König, M. Hörteis, G. Hahn, En. Proc. 38 (2013) 720.
[13] X. Li, L. Tao, Z. Xia, Z. Yang, J. Dong, W. Song, B. Zhang, R. Sidhu, G. Xing, Proc. 37th IEEE PVSC (2012) 1073.
[14] H. Haverkamp, A. Dastgheib-Shirazi, B. Raabe, F. Book, G. Hahn, Proc. 33rd IEEE PVSC (2008) 430.
[15] W. Kolasinski, Current Opinion in Solid State and Materials Science 9 (2005) 73.

[16]D.E. Kane, R.M. Swanson, Proc. 18th IEEE PVSC (1985) 578.